processes

MDPI

Article

Effect of Dry-Wet Cycling on the Mechanical Properties of Rocks: A Laboratory-Scale Experimental Study

Xiaojie Yang [1,2], Jiamin Wang [1,2,*], Dinggui Hou [3], Chun Zhu [1,*] and Manchao He [1]

1 State Key Laboratory for Geomechanics and Deep Underground Engineering, China University of Mining and Technology, Beijing 100083, China; xyang@cumtb.edu.cn (X.Y.); hemanchao@163.com (M.H.)
2 School of Mechanics and Civil Engineering, China University of Mining and Technology, Beijing 100083, China
3 Construction Engineering Department, North China Institute of Aerospace Engineering, Langfang 065000, China; houdinggui@126.com
* Correspondence: bqt1700620037@student.cumtb.edu.cn (J.W.); zhuchun17@mails.jlu.edu.cn (C.Z.)

Received: 12 September 2018; Accepted: 16 October 2018; Published: 19 October 2018

Abstract: Taking Nanfen open-pit iron mine in Liaoning Province as the engineering background, this study analyzes the effect of water-rock circulation on the mechanical properties of rock through a combination of macro-mechanical experiments and microstructure tests in the laboratory. Uniaxial compression experiments and acoustic wave tests are used to determine the degradation law of the mechanical properties of chlorite under the periodic action of water. The experimental results show that dry-wet cycles have a continuous and gradual effect on the rock sampled: Its uniaxial compressive strength, elastic modulus, and acoustic velocity all decrease gradually with an increase in the number of cycles. After 15 wet-dry cycles, the uniaxial compressive strength and elastic modulus of the rock decreased by 34.21% and 44.63%, respectively. Electron microscope scans of the rock indicate that the particle size, characteristics, and pore distribution at the rock surface had changed significantly after water-rock interaction. Finally, a drainage system and sliding force monitoring devices have been arranged at the mine site that can effectively reduce the impact of water-rock interaction on the stability of the mine. This combination of macro-experiments and micro-analysis allowed the weakening effect of dry-wet cycles on slope rock to be studied quantitatively, providing a theoretical reference for stability evaluation in geotechnical engineering.

Keywords: water-rock interaction; dry-wet cycles; slope stability; laboratory experiment; mechanical properties

1. Introduction

Geotechnical engineering problems have been on the increase in recent years in concert with the continuous expansion of geotechnical projects such as water conservancy projects, deep coal mines, and slope projects [1,2]. Along with environmental impacts, geotechnical engineering problems commonly relate to geotechnical stability, such as foundation stability, slope stability, tunnel stability, etc. [3,4] Therefore, it is essential to evaluate and ensure rock mass stability in order to solve geotechnical engineering problems effectively. In addition to the basic properties of the rock mass such as its hardness and integrity, water, rock structure, stress state, and planes of weakness in the rock also have important effects on the stability of the rock mass. Among these, water is the most common and important factor affecting rock mass stability due to the prevalence of rock-water interaction and the widespread existence of water in nature [5]. According to incomplete statistics, water plays an important role in more than 90% of cases of rock slope instability, 60% of mine accidents,

and about 35% of water conservancy accidents [6]. From the perspective of geotechnical engineering, the interaction between water and rock is essentially a continuous physical, chemical, and mechanical process. This process changes the physical and mechanical parameters of the rock, thus causing a loss of stability in geotechnical engineering contexts [7].

Water-rock interaction is an important component of geotechnical engineering stability evaluations, and its study has been at the frontier of this field in recent years [8,9]. Rock is a porous material mainly composing a solid skeleton and pores. The rock is made up of many kinds of minerals, and many cracks and holes are formed in the process of diagenesis [10,11]. Rock is a non-uniform and non-linear material with a discontinuous interior surface inside, and the pore distribution within the rock shows randomness, diversity, and variability. An increase in the microstructural non-uniformity and discontinuity in a rock equates to damage that will inevitably lead to changes in the rock's macro-mechanical properties, thus adversely affecting overall geotechnical stability. Most studies of the influence of water on the mechanical properties of soft rock, both at home and abroad, focus on the changes in the physical and chemical properties of the rock and the law governing strength reduction after water absorption [12–14]. However, the interaction between rock and water occurs not only through soaking and water absorption. Many rocks in practical projects must also face a more complicated and changeable natural environment, such as frequent rainfall and evaporation, rise and fall of underground water level, fluctuation of the water surface in a reservoir area, etc. [15,16]. Periodic water-rock interaction is a kind of "repeated softening" for rocks [17–19]. The consequence of these processes is that the rock repeatedly absorbs and loses water, putting the rock through a frequent alternation of dry and wet cycles. The weakening effect of these cycles on rock is often stronger than that of being soaked in water for a long time and thus a serious influence on the long-term stability of rock masses in engineering. Therefore, further study is required into the influence law of repeated dry and wet cycles on the mechanical properties, mode of crack propagation, and failure mechanism of rock. A systematic and in-depth study of microstructural damage, macro-deformation, and strength deterioration of rock under dry-wet cycles will help to fundamentally establish the mechanism by which rocks are weakened by repeated water-rock interaction.

The Nanfen open-pit iron mine is located in Nanfen District, Benxi City, Liaoning province and is the largest single open-pit mine in Asia [20,21]. Water is an indispensable and important component of a complex geological environment. It can interact with rock through pores, cracks and weak structural planes in the rock mass, thus weakening the mechanical properties and damaging the microstructure of the rock mass. This is particularly an issue for open pit mine slopes, which are very deformable and dynamic. Thus, slope stability problems caused by rainfall and groundwater level rise and fall have become a hot research topic in the field of geotechnical mechanics [22–24]. The mechanical experiment of rock under water-rock interaction can help us to obtain the change law of rock's mechanical properties affected by water at the laboratory scale. For example, uniaxial compression test and acoustic wave test of rock under different dry-wet cycles can obtain the attenuation law of uniaxial compression strength, elastic modulus, and acoustic wave velocity of rock with the number of cycles. In addition, the development of scanning electron microscope makes the quantitative research methods of rock microstructure become more and more mature. Through the macroscopic mechanical experiment and microscopic structure analysis of rock, it is easy to find the deterioration process of slope rock under the different numbers of dry-wet cycles, which can provide a theoretical reference for analyzing the stability of open-pit slope rock in a periodic water environment and the implementation of waterproof engineering.

2. Materials and Methods

2.1. Rock Sample Selection

The Nanfen open-pit iron mine exploits a sedimentary metamorphic iron ore layers [25]. The mining area has an undulating topography, and the footwall slope of the mining area is rocky,

with weak development of layering, characteristics that make it easy for geological disasters such as collapse and landsliding to occur. A huge amount of rock stripping and mining is carried out in this mine every year. Due to the characteristics of the terrain and the comprehensive influence of mining, many large-scale landslides have formed on the downdip part of the lower slope, threatening safe production in the mining area. On 3 August 2012, Nanfen open-pit iron mine was hit by heavy rain from typhoon "Dawei", which resulted in large-scale cracks, collapses, and landslides on the slope, as shown in Figure 1a,b. A large area that could potentially slide has been created, which seriously threatens the normal safe production of the mine.

(**a**) (**b**)

Figure 1. Landslides and collapses caused by rainfall. (**a**) local landslide; and (**b**) overall collapse

Rainfall and slope sliding force in the mining area were monitored in real time to study the correlation between deformation and failure of the slope and rainfall in Nanfen open pit mine, as well as to predict the landslide trend. Statistical analysis was carried out on rainfall and significant changes in the slope sliding force at Nanfen open-pit mine, as shown in Table 1 and Figure 2. Changes in sliding force that are greater than or equal to 100 kN within 24 h are considered significant, and heavy rain is defined, as per the rainfall standard set by the Chinese meteorological department, as above 50 mm per day.

Table 1. Statistics on rainfall and sliding force changes in Nanfen open-pit iron mine (From November 2010 to November 2012).

Month	1	2	3	4	5	6	7	8	9	10	11	12
Days of rain	0	0	0	18	11	38	30	37	25	26	3	0
Days of heavy rain	0	0	0	0	2	6	8	9	9	4	0	0
Number of significant changes in sliding force	1	0	0	0	0	4	6	15	2	2	0	0

The statistical data show that rainfall often occurs before a period of significant change in sliding force. Most such changes occur in a month when there is frequent rainfall, especially in months when there is frequent heavy rainfall, which shows that rainfall is an important factor for slope instability. Rainfall will induce landslides and change the physical and mechanical parameters of slope rock and soil. Due to the softening effect of rainwater, the rock and soil will become saturated, the gravity density will increase, and the shear strength and deformation modulus will decrease [26]. The continuous interaction of water and rock will cause cracks in the rock mass to expand and penetrate, eventually leading to rock destruction and slope instability. Sampling was mainly concentrated in chlorite on 478 m steps on the footwall of the slope. A portable knapsack type core drilling rig was used for shallow sampling of complete rock samples. This device is simple and convenient to carry, flexible, and highly efficient. After drilling and taking samples at the site, the samples were sealed in wax and put into a portable sample collection box for storage and transportation. The processed rock samples are cylinders with a diameter of 50 mm and a height of 100 mm ($\pm$1 mm). Rock samples with relatively similar wave velocities were identified non-metallic ultrasonic detectors and screened out as experimental rock samples.

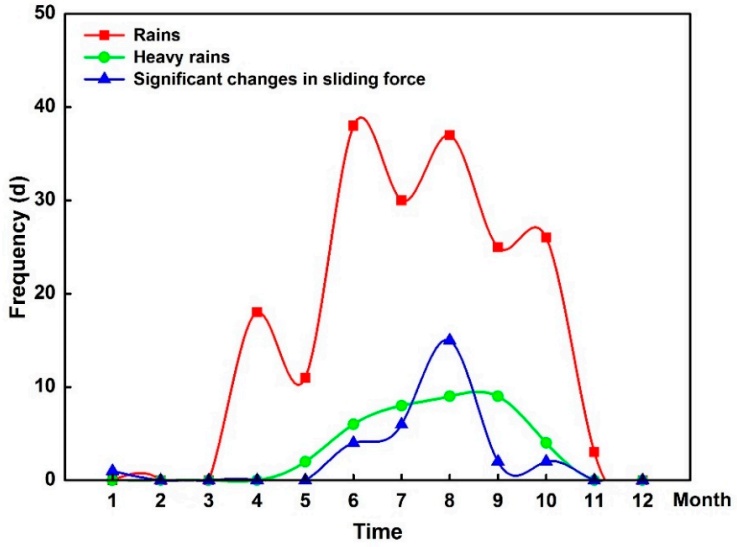

Figure 2. Frequencies of significant changes in sliding force, rain, and heavy rain during two years.

2.2. Experimental Design of Dry and Wet Cycling

Dry-wet cycles were simulated in the laboratory to study their effect on the mechanical properties and microstructure of rock. Taking into account the operability of the dry-wet cycle experiment and the actual situation in the field, the "water saturation-natural air drying" method was implemented for each cycle to avoid the effect that the high temperature used in the oven drying method would have on rock properties and microstructure. The rock samples were divided into 6 groups, 3 in each group, and were subjected to 0 cycles (representing the natural state), 1 cycle, 3 cycles, 6 cycles, 10 cycles, and 15 cycles, respectively. A uniaxial compression test, acoustic wave test, and scanning electron microscope test was carried out on each rock sample. Rock samples were saturated by placing the sample in water, controlling the water level at the 1/4 L, 1/2 L, 3/4 L, and 1 L planes of the sample height L in sequence and soaking them for 2 h at each of these levels. The sample was then completely immersed in water and left to absorb it for 48 h before being taken out. Finally, the surface water was gently absorbed with tissue paper, and the sample was weighed. In order to maintain the uniformity of the water absorption process, the height between the upper surface of the rock sample and the water surface was controlled to be 10 cm in each complete soaking. Rock sample drying was carried out by natural air drying, placing the rock sample in a windless room at 26 degrees Celsius for more than 7 d until the mass became constant.

2.3. Uniaxial Compression Tests

The purpose of uniaxial compression testing of rock is to determine its uniaxial compressive strength, elastic modulus, Poisson's ratio and other parameters of rock [27]. The uniaxial compression experiment was carried out on an XTR01 microcomputer servo-controlled rock compression testing machine (Changchun, China), it is a stiff testing machine specially used for testing materials such as rocks and concrete. This device can automatically record the applied load and the axial and radial deformation values of the rock during the experiment prior to destruction. The stress-strain curve of the rock can be drawn on the basis of the collected data, from which the uniaxial compressive strength of the rock can be obtained.

2.4. Acoustic Velocity Tests

All rock masses in the natural environment contain various joints, fissures, and other structural planes. The deformation of these structural planes in the rock mass under the action of external forces will cause reflection, refraction, diffraction, scattering, and other phenomena during elastic

wave penetration, which will affect the propagation path of elastic waves in the rock mass [28–30]. Acoustic wave detection technology analyzes the structural characteristics of a rock mass by using the wave characteristics of elastic waves that pass through it [31]. The acoustic wave velocity test adopted by this study uses an MC-6310 nonmetal ultrasonic detector (Beijing, China). The experimental process is shown in Figure 3a,b. The device is used to excite elastic waves of a certain frequency inside the rock. Elastic waves propagate inside the rock in the form of transverse waves and longitudinal waves, which are transmitted and received by probes at both ends. By analyzing the recorded wave signals, the mechanical properties of the rock and its internal defects are determined. The relationship between the wave velocity value for the rock and the number of dry-wet cycles was analyzed by testing the longitudinal and transverse wave velocities in the rock samples after different numbers of water saturation cycles.

(**a**)

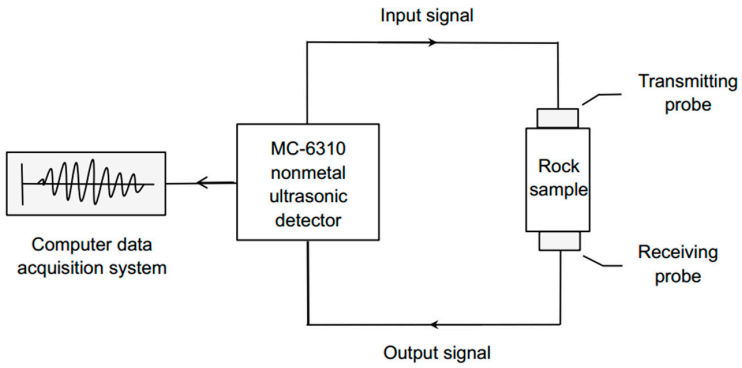

(**b**)

Figure 3. Acoustic wave testing. (**a**) experimental process of wave velocity test in rock; and (**b**) schematic diagram of the acoustic wave test.

2.5. Scanning Electron Microscope Test

The instrument used for scanning electron microscope testing was the Hitachi SU8010 electron microscope made in Tokyo, Japan. The rock sample was prepared as a test block 1 cm^2 × 0.5 cm in size. After pre-treatments such as grinding and drying, the experimental sample was bonded to the sample pile with conductive adhesive, and a layer of gold film was plated to the surface of the sample. It was then put into the sample room for scanning, the scanning result was observed, and a picture was extracted [32,33].

3. Results and Analysis

In order to conveniently illustrate changes in the mass of rock during the dry-wet cycling process, the change in the mass of one rock sample in the first wet-dry cycle is plotted in Figure 4. The four stages a, b, c, and d, in the figure correspond to rock been soaked in water at water levels of 1/4 L, 1/2 L, 3/4 L, and 1 L, respectively. These four stages lasted for 8 h in total, and the rock mass increased from 564.4 g to 565.146 g. After 56 h of soaking, the final saturated rock mass was 565.28 g, the water absorption was 0.755 g, and the ratio of absorbed water to rock was 0.134%. In the process of air-drying, the mass of the rock was measured after 5 d (i.e., after the 176th hour) and 7 d (i.e., after the 224th hour), and the values were found to be equal, indicating that air-drying for 7 d can guarantee the complete drying of the rock. The mass of the dehydrated rock is 564.28 g, which is 0.12 g lower than the initial state; the mass loss ratio is 0.024%. The mass loss ratio of rock is defined as the ratio of the lost mass of rock to the initial mass of rock. The loss curve of rock mass up to 15 cycles is plotted in Figure 5.

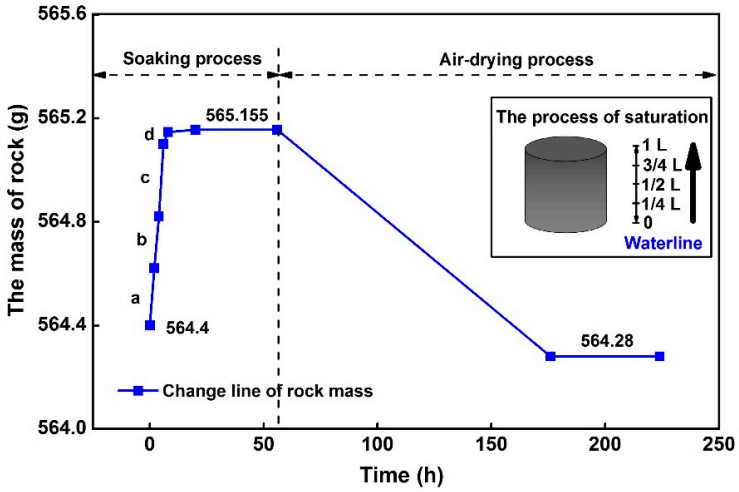

Figure 4. Mass change of one of the rock samples after the first wet-dry cycle.

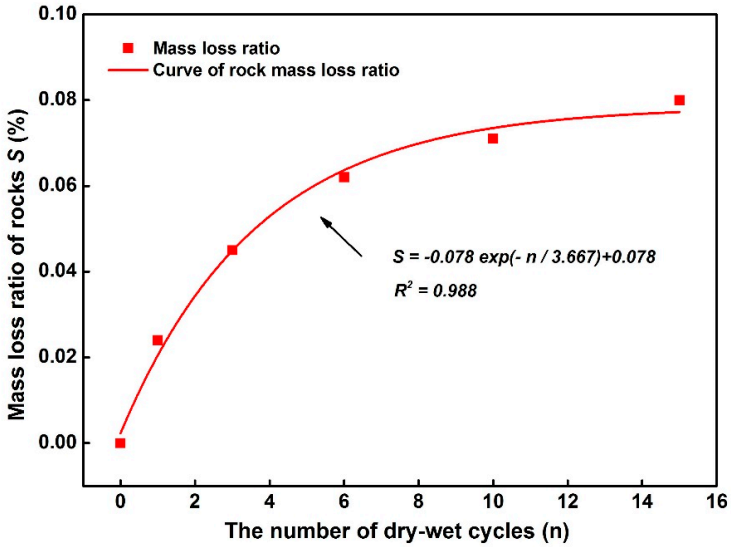

Figure 5. The relationship between rock mass loss ratio and the number of dry-wet cycles.

As can be seen from Figure 5, the mass loss ratio of the rock increases with an increase in the number of dry-wet cycles. After the first three wet-dry cycles, the mass loss ratio of rock is 0.045%, while after 15 cycles, the mass loss ratio increased to 0.08%. This increase is more rapid in the early

stages and decelerates in the later stages. According to fitting analysis conducted with Origin software, the two variables are exponentially correlated with the fitting equation:

$$S = -0.078\, exp(-n/3.667) + 0.078,\ R^2 = 0.988 \quad (1)$$

where S represents the mass loss ratio of the rock (%), that is, the ratio of the lost mass of rock to the initial mass, n is the number of dry and wet cycles, and R^2 represents the correlation coefficient between the mass loss ratio of the rock and the number of dry-wet cycles.

Chlorite is an aluminosilicate mineral, and some of the rock debris is physically and chemically unstable, making the rock easily mechanically eroded, transported, and altered in a water-bearing environment. Therefore, from a microscopic point of view, the damage to the rock mass is mainly caused by the migration and diffusion of debris and the dissolution of feldspar and other particles under the influence of repeated wet-dry cycles. This changes the physical structure, creating secondary pores. One of the main macroscopic manifestations of this phenomenon is the mass loss of the rock samples after dry-wet cycling.

3.1. Analysis of Uniaxial Compression Test Results

The uniaxial compression tests allowed stress-strain curves for rock samples subjected to different numbers of dry-wet cycles to be obtained, as well as the uniaxial compressive strength, elastic modulus and other parameters of the rocks. In order to explore the influence of dry-wet cycles on rock strength and deformation, strength loss percentage was defined as the degree of attenuation of uniaxial compressive strength under dry-wet cycling, i.e., $(\sigma_{t0} - \sigma_{ti})/\sigma_{t0} \times 100\%$, and the elastic modulus loss percentage was defined as the degree of attenuation of the elastic modulus under dry-wet cycles, i.e., $(E_0 - E_i)/E_0 \times 100\%$. The statistical results for the average uniaxial compressive strength and elastic modulus of chlorite and their degree of attenuation after different numbers of dry-wet cycles are shown in Table 2.

Table 2. Statistics of experimental results for rock uniaxial compression.

Cycles	Uniaxial Compressive Strength σ_t		Elastic Modulus E	
	Average Value (MPa)	Attenuation Degree D_1 (%)	Average Value (GPa)	Attenuation Degree D_2 (%)
0	102.85	0	31.12	0
1	96.38	6.29	29.83	4.15
3	89.79	12.70	27.13	12.82
6	80.84	21.40	24.86	20.12
10	73.28	28.75	20.94	32.71
15	67.66	34.21	17.23	44.63

It can be seen from Table 2 that the average uniaxial compressive strength and average elastic modulus of the chlorite decrease with an increase in the number of dry-wet cycles. The cumulative degrees of attenuation of the average uniaxial compressive strength and average elastic modulus reach 34.21% and 44.63%, respectively, after 15 dry-wet cycles. After more than 10 cycles, the degree of attenuation of the average elastic modulus of the chlorite gradually exceeds the degree of attenuation of the uniaxial compressive strength, indicating that there is more significant degradation of the average elastic modulus of rock than of its uniaxial compressive strength under the action of multiple dry-wet cycles. Curves for the average uniaxial compressive strength and elastic modulus of the rocks versus the number of dry-wet cycles, together with their degree of attenuation, are given in Figures 6 and 7, respectively.

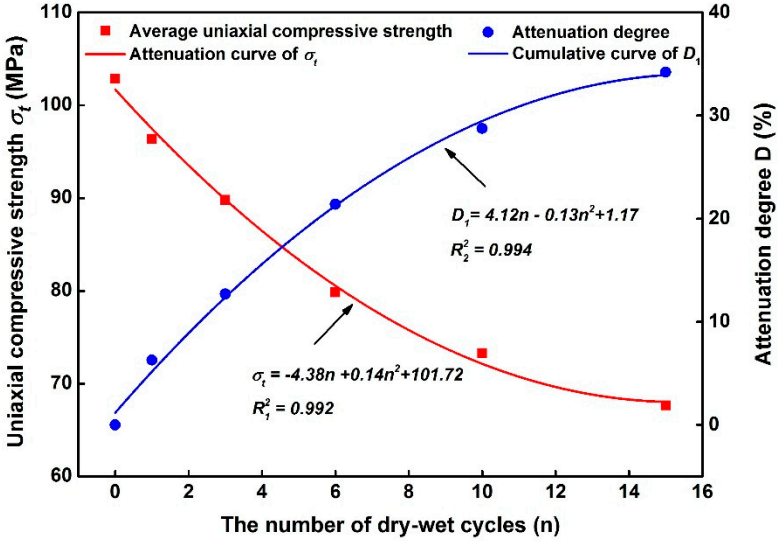

Figure 6. The changes of average uniaxial compressive strength of rock and its degree of attenuation with the number of dry-wet cycles.

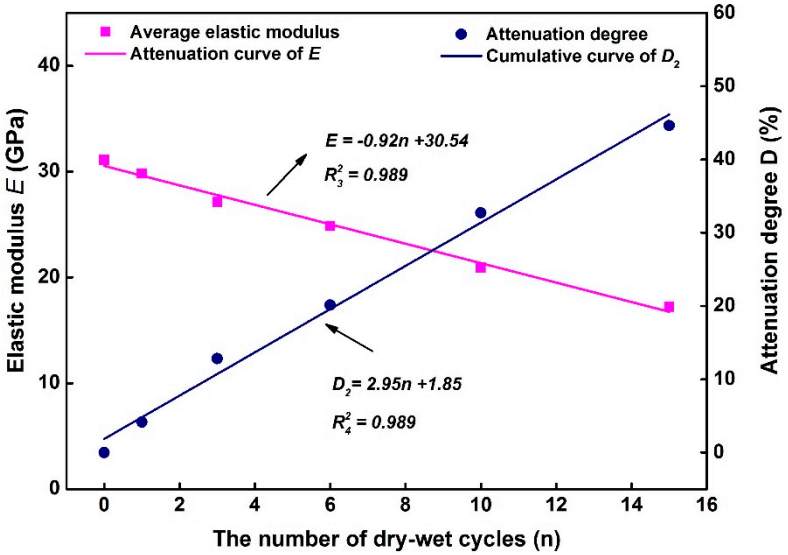

Figure 7. The changes of average elastic modulus of rock and its degree of attenuation with the number of dry-wet cycles.

As can be seen from Figure 6, the average uniaxial compressive strength of the chlorite gradually decreases with an increase in the number of dry-wet cycles, from 102.85 MPa in the initial state to 67.66 MPa after 15 dry-wet cycles. The decrease is most quickly in the early stages and more slowly in the later stages. Correspondingly, the degree of attenuation of average uniaxial compressive strength gradually increases with an increase in the number of dry-wet cycles, from 0% in the dry state to 34.21% after 15 dry-wet cycles. The attenuation trend in the average elastic modulus of the rock shows a similar variation trend, as shown in Figure 7, which is basically uniform and approximately linear. After 15 cycles, the average elastic modulus of the rock is about 45% lower than it was initially, from 31.12 GPa to 17.23 GPa. In order to further quantitatively analyze the softening effect of dry-wet cycling on rock, a fit to the data in the figure was obtained using the function provided by Origin software. The relationship between the average uniaxial compressive strength of rock and the number of dry-wet cycles is found to be well-expressed as a good polynomial function, with the fitting equation

$$\sigma_t = -4.38n + 0.14n^2 + 101.72,\ R_1^2 = 0.992 \quad (2)$$

where σ_t is the uniaxial compressive strength of the rock (MPa), n is the number of dry-wet cycles, and R_1^2 represents the correlation coefficient between the uniaxial compressive strength of the rock and number of dry-wet cycles.

Fitting analysis with Origin software indicates that the average elastic modulus of the rock and the number of dry-wet cycles have a strong linear relationship, with the fitting equation

$$E = -0.92n + 30.54,\ R_3^2 = 0.989 \quad (3)$$

where E is the elastic modulus of the rock (GPa), and R_3^2 represents the correlation coefficient between the uniaxial compressive strength of the rock and the number of dry-wet cycles.

Thus, the uniaxial compressive strength and elastic modulus of the rock decreases with an increase in the number of dry-wet cycles, which shows that dry-wet cycling has a substantial damaging effect on the rock's mechanical strength. The characteristics of the rock itself and the influence of different environments and stress conditions lead to different rock masses showing different failure modes. Figure 8 presents images of chlorite samples from Nanfen destroyed by uniaxial compression tests after different numbers of dry-wet cycles. From left to right, the rock samples in the images were subjected to 0, 1, 3, 6, 10, and 15 dry-wet cycles.

Figure 8. Images of failure in rock samples after different numbers of dry-wet cycles.

Rock failure characteristics are affected by numerous factors such as mineral composition, distribution of structural planes, and the loading and stress conditions in the experimental process. It was clearly seen during the uniaxial compression tests that the post-loading failure surfaces of rocks in dry state and after one dry-wet cycle ran through the entire longitudinal axis of the rock sample. The failures were accompanied by ringing noise characteristics of brittle, tensional failure. With an increase in the number of dry-wet cycles, the characteristics of the brittle failure transitioned from strong to weak. Fissures developed that ran through the weak surfaces of the rock, and friction-induced pulverization appeared at the failure surface, a characteristic of weak surface shear failure. The sound emitted by rock failure became more complex and quieter. The failure characteristics of rocks gradually changed from brittle failure to shear failure with an increase in the number of dry-wet cycles, indicating that dry-wet cycles have a significant impact on the failure characteristics of chlorites.

3.2. Experimental Analysis of Acoustic Wave Velocity Tests

Acoustic velocity tests, including an axial transverse wave test and longitudinal wave test, were conducted the rock samples with an MC-6310 nonmetal ultrasonic detector (Beijing, China) after different numbers of dry-cycles tests to determine the degree of microscopic damage in the rocks. The experimental results are shown in Table 3, and the relationship between the acoustic wave velocities in the rocks and the number of dry-wet cycles is shown in Figure 9.

Table 3. Experimental results of acoustic wave velocity tests.

Cycles	Longitudinal Wave Velocities (m/s)	Absolute Reduction (m/s)	Relative Reduction (%)	Transverse Wave Velocities (m/s)	Absolute Reduction (m/s)	Relative Reduction (%)
0	4358	0	0	2812	0	0
1	4346	12	0.28	2768	44	1.56
3	4298	60	1.34	2706	106	3.77
6	4175	183	4.20	2623	189	6.72
10	3963	395	9.06	2524	288	10.24
15	3752	606	13.91	2446	366	13.02

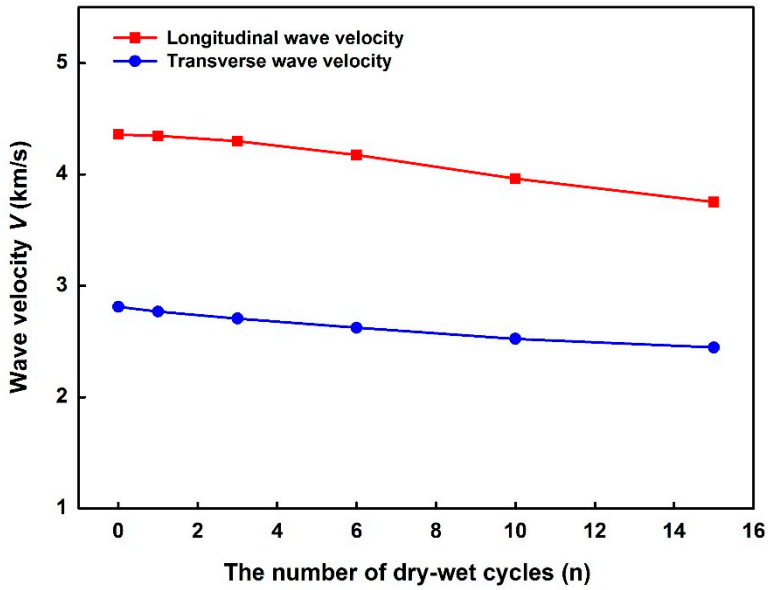

Figure 9. The relationship between the average acoustic velocity in the rocks and the number of dry-wet cycles.

Acoustic wave velocity testing is an effective method for studying the mechanical properties and structural compactness of rock. As can be seen from Table 3, the propagation speed of acoustic waves in solids depends on the direction of particle vibration. The propagation speed of longitudinal waves in rocks is about 1.55 times greater than that of transverse waves. The curves of longitudinal wave velocity and transverse wave velocity versus the number of dry-wet cycles in Figure 9 allow it to be seen intuitively that both longitudinal wave velocity and transverse wave velocity have an attenuation trend with an increase in the number of periodic dry-wet cycles. From the 0 to the 15th cycle, the longitudinal wave velocity decreased by 606 m/s, a decrease of 13.91%, and the transverse wave velocity decreased by 366 m/s, a decrease of 13.02%. The propagation speed of acoustic waves in rock will be greatly affected by the integrity and pore density of the rocks. Chlorite is a hard rock, with high strength and poor water absorption. Acoustic waves propagation through rocks diffract when fissures and pores are encountered, resulting in an increase in the propagation distance and a decrease in the wave velocity. With an increase in the number of dry-wet cycles, the cracks gradually develop and expand inside the rock mass and many new micro-cracks will be formed. This gradual increase in the porosity of the rock explains the decrease in wave velocity. Therefore, the axial wave velocity of rock samples can be used as effective indicators of crack growth inside rock, and the rate of decrease in the acoustic wave velocity can be used to characterize differences in the degree of damage between rocks.

3.3. Analysis of Scanning Electron Microscope (SEM) Images

After obtaining scanning electron microscope images of the rocks after different numbers of dry-wet cycles, an initial observation of the images was carried out with the naked eye. In order

to compare the influence of different numbers of dry-wet cycles on the pore structures of the rocks, a consistent magnification was used to generate the scanning electron microscope images. 100×-magnified SEM images of chlorite that have undergone different numbers of cycles are shown in Figure 10. After several dry-wet cycles, there are obvious changes to the characteristics shown in the SEM images and the structure of the rock sample.

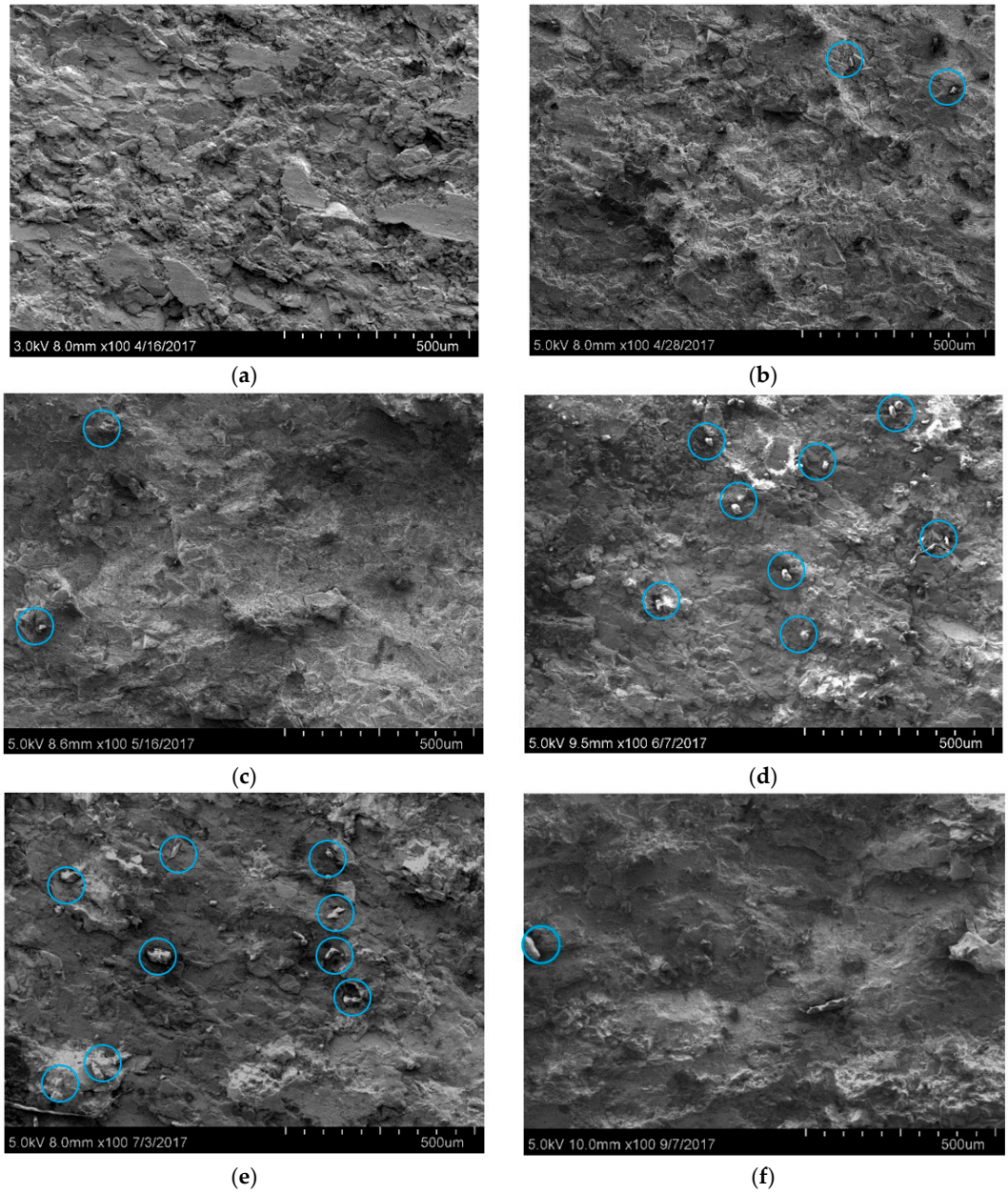

Figure 10. SEM images of rocks after different numbers of dry-wet cycles. (**a**) zero cycles; (**b**) one cycle; (**c**) three cycles; (**d**) six cycles; (**e**) ten cycles; and (**f**) fifteen cycles.

An increase in the number of dry-wet cycles leads to gradual damage accumulation in the rocks. The pore types of chlorites are mainly mineral cleavage crevices and intergranular micropores between clay mineral. Chlorites have a much higher degree of water absorbency than rocks such as sandstone and mudstone. As can be seen from Figure 10, without the action of dry-wet cycles, the rock particles are clear in outline and evenly distributed, and the microstructure is homogeneous and compact. The particles are mainly flat and massive; the macro-mechanical properties of the rocks are also good at

this time. After several dry-wet cycles, the microstructures of the rocks are no longer compact and flat, the particles begin to become disordered, and some flaky, curling particles appear. Crystal precipitation also occurs on the surface of the rock (in blue circles in the Figure 10) and gradually increases with an increase in the number of dry-wet-cycle times. After fifteen cycles, fine mud particles have accumulated at the surfaces of the rocks due to water-rock interaction, making them uniform and smooth again. The microscopic structure and morphology of the rock have changed completely, as compared with the chlorites in a dry state, at this time.

Based on the results of the rock mechanics experiments and analyses of microscopic SEM images, we can conclude that water molecules penetrate into the interior of the rock it is soaked in water, water-soluble particles are dissolved by the water, and fine cuttings are stripped off, leaving behind pore fissures. The expansion of pores and fissures creates conditions that are more conducive to the penetration of water molecules into the rock and reduces the cohesion and binding force between rock particles. The microscopic damage to the rock develops continuously, which is exhibited macroscopically in a decrease in mechanical parameters such as the compressive strength, elastic modulus, and acoustic wave velocity. The accumulation of physical, chemical and mechanical damage caused by rock-water interaction is the main reason that slope stability is affected and the deformation and destruction of engineering rock mass occur. Furthermore, rainfall and evaporation and the rise and fall of the groundwater level will subject the rock mass of a slope to dry-wet cycles for a long time, which will accelerate the accumulation of damage.

4. Prevention Measures of Slope Instability

Rainfall is an important cause of hazardous landslides in Nanfen open-pit iron mine slopes. The effect of rainfall can be mitigated by a variety of slope stability control measures including surface drainage engineering, underground drainage engineering, back pressure engineering, weight reduction engineering, and river engineering [34–36]. For landslides with relatively fixed boundaries and a small traction range, permanent interception, and drainage to outside the landslide range can be put in place. The type of surface drainage installed within the landslide range will depend on the specific situation. When the landslide is already in an unstable state, the drainage system should be designed to be temporary, with less investment made and with an emphasis on timely maintenance. Interception ditches and drains are also very effective for intercepting and draining water at the surface. The results of the current study confirm that if effective measures are not taken to drain fissure water on the slope, the strength of the soil and rock mass will be reduced, a landslide will develop more quickly, and the safety and sustainable mining of the open-pit mine will be seriously threatened. One of the ultimate goals of the slope drainage project at Nanfen open-pit iron mine is to discharge surface water and groundwater from the mining site to the region outside the stope. The terrain and rock structure of the stope mean that the drainage pipe can be connected to the drainage interception ditch through a sand basin to form a complete water defense system, as shown in Figure 11.

Figure 11. Pipe draining of rainwater and groundwater away from Nanfen open-pit mine slope.

Deep drainage holes enable the effective and timely discharge of fissure water in the deep rock mass and play a directly beneficial role in maintaining the stability of the slope. When there is no drainage system, rainwater will penetrate into the slope along cracks and form runoff at the surface, which will seriously affect the stability of the local slope. In addition, because the dangerous slope at Nanfen open-pit mine is about 400 m in length, 432 m in height, and 172,800 m^2 in area, joints and fissures are developed, and geological conditions are complex, rainfall and the rise and fall of groundwater level have a major impact on the slope. On the basis of extensive research, our organization has installed sliding force monitoring points and rainfall monitoring points on the footwall slope of Nanfen open-pit iron mine to enable 24-h intelligent monitoring of the hydrogeological environment. This monitoring method allows the comprehensive analysis of slope stability and prediction of slope evolution [37,38]. The installation of drainage system, monitoring, and an early warning system for rainfall and the sliding force of the slope are of great significance for forecasting and analyzing rainfall-induced landslides.

5. Conclusions

Based on the engineering background of Nanfen open-pit iron mine in Liaoning province, this study investigated the mechanical properties of rocks subjected to water-rock circulation through macroscopic mechanical experiments, microstructure tests, and theoretical analysis. Periodic water circulation due to rainfall, evaporation and the fluctuation of groundwater level was simulated in the laboratory, and valuable data were obtained regarding its effect on the mechanical property parameters of these Nanfen chlorite rocks.

Dry-wet cycling is found to accelerate the generation and expansion of cracks in the rock, resulting in a decrease in rock strength. The uniaxial compressive strength of the rock decreases with an increase in the number of dry-wet cycles, showing a large decrease in the early stages and a more gradual decrease with continued cycling. This change trend follows the polynomial function "$\sigma_t = -4.38n + 0.14n^2 + 101.72$". However, there is a linear relationship between the attenuation of the elastic modulus of the rock and the number of dry-wet cycles. Brittle failure in the rock shows a transition from exhibiting the characteristics of strong rock to those of weak rock with an increase in the number of cycles. Acoustic wave testing shows that both longitudinal wave velocity and transverse wave velocity are attenuated to a certain extent under the influence of water-rock interaction. The attenuation rates of longitudinal wave velocity and transverse wave velocity are 13.91% and 13.02%, respectively. The two have a very similar attenuation trend, but the absolute attenuation of longitudinal wave velocity is much greater than that of transverse wave velocity. In the early stages of water absorption, the chlorite itself is hard, strong, and has poor water absorbency. The interaction between water and rock causes cracks in the rock mass to gradually form and expand. This increase in porosity leads to the decrease in wave velocity.

Based on the theory of rock damage mechanics, the microstructure of rock samples was examined by SEM after different numbers of dry-wet cycles. The images show that the rock surface was initially compact and flat, with clear particle outlines. With an increase in the number of dry-wet cycles, crystalline minerals continuously precipitated onto the rock surface and gradually became cohesive. Until after the 15th cycle, the microstructure and morphology of the rock had completely changed, showing a muddy state. The surface was leveled again.

To sum up, there is cumulative physical, chemical, and mechanical damage to the rock mass in Nanfen open-pit iron mine due to rainfall and groundwater. The stability of the rock mass will be gradually weakened over a long period of time, inevitably leading to the deformation and destruction of the mining area slope. Feasible drainage measures should be taken, and early warning and monitoring of slope stability should be strengthened to ensure that mines are mined safely and that lives and property of the workers are protected. It is hoped that further numerical simulation can be conducted and more rock samples can be selected for comparative analysis in the future to further quantify the influence of dry-wet cycling on the mechanical properties of slope rock.

Author Contributions: X.Y. and J.W. designed and performed the experiments, they contributed equally to this work. D.H. and C.Z. analyzed the data; M.H. contributed experimental materials and conditions; X.Y. provided funding; J.W. wrote and edited the paper.

Funding: This research was funded by the National Natural Science Foundation of China, grant number 41672347 and Natural Science Foundation of Beijing Municipality, grant number 8142032.

Acknowledgments: The authors would like to express sincere appreciation to the editors and reviewers for their time and effort to review this paper and provide valuable comments.

Conflicts of Interest: The authors declare no conflict of interest.

References

1. Su, Y.H.; Fang, Y.B.; Li, S.; Su, Y.; Li, X. A one-dimensional integral approach to calculating the failure probability of geotechnical engineering structures. *Comput. Geotech.* **2017**, *90*, 85–95. [CrossRef]
2. Wu, X.Z. Trivariate analysis of soil ranking-correlated characteristics and its application to probabilistic stability assessments in geotechnical engineering problems. *Soils Found.* **2013**, *53*, 540–556. [CrossRef]
3. Yang, J.; Tao, Z.G.; Li, B.L.; Yang, G.; Li, H.F. Stability assessment and feature analysis of slope in Nanfen Open Pit Iron Mine. *Int. J. Min. Sci. Technol.* **2012**, *22*, 329–333. [CrossRef]
4. Ma, C.Q.; Wang, P.; Jiang, L.S.; Wang, C.S. Deformation and control countermeasure of surrounding rocks for water-dripping roadway below a contiguous seam goaf. *Processes* **2018**, *6*, 77. [CrossRef]
5. He, M.C.; Sun, X.M.; Zhao, J. Advances in interaction mechanism of water (gas) on clay minerals in China. *Int. J. Min. Sci. Technol.* **2014**, *24*, 727–735. [CrossRef]
6. Wu, Y.Q.; Zhang, N.Y. *An Introduction to Rock Mass Hydraulics*; Southwest Jiaotong University Press: Chengdu, China, 1995.
7. Zhao, Z.H.; Guo, T.C.; Ning, Z.Y.; Dou, Z.H.; Dai, F.; Yang, Q. Numerical modeling of stability of fractured reservoir bank slopes subjected to water-rock interactions. *Rock Mech. Rock Eng.* **2018**, *51*, 2517–2531. [CrossRef]
8. Phan, T.T.; Vankeuren, A.N.P.; Hakala, J.A. Role of water-rock interaction in the geochemical evolution of Marcellus Shale produced waters. *Int. J. Coal Geol.* **2018**, *191*, 95–111. [CrossRef]
9. Jiang, J.W.; Xiang, W.; Rohn, J.; Zeng, W.; Schleler, M. Research on water–rock (soil) interaction by dynamic tracing method for Huangtupo landslide, Three Gorges Reservoir, PR China. *Environ. Earth Sci.* **2015**, *74*, 557–571. [CrossRef]
10. Zhang, X.M.; Tahmasebi, P. Micromechanical evaluation of rock and fluid interactions. *Int. J. Greenh. Gas Control* **2018**, *76*, 266–277. [CrossRef]
11. Zhu, Y.P. A micromechanics-based damage constitutive model of porous rocks. *Int. J. Rock Mech. Min. Sci.* **2017**, *91*, 1–6. [CrossRef]
12. Hao, R.Q.; Li, J.T.; Cao, P.; Liu, B.; Liao, J. Test of subcritical crack growth and fracture toughness under water-rock interaction in three types of rocks. *J. Cent. South Univ.* **2015**, *22*, 662–668. [CrossRef]
13. Wong, L.N.Y.; Maruvanchery, V.; Liu, G. Water effects on rock strength and stiffness degradation. *Acta Geotech.* **2016**, *11*, 713–737. [CrossRef]
14. Hashiba, K.; Fukui, K. Effect of water on the deformation and failure of rock in uniaxial tension. *Rock Mech. Rock Eng.* **2015**, *48*, 1751–1761. [CrossRef]
15. Doostmohammadi, R.; Moosavi, M.; Mutschler, T.; Osan, C. Influence of cyclic wetting and drying on swelling behavior of mudstone in south west of Iran. *Environ. Geol.* **2009**, *58*, 999. [CrossRef]
16. Zhao, Z.H.; Yang, J.; Zhang, D.F.; Peng, H. Effects of wetting and cyclic wetting–drying on tensile strength of sandstone with a low clay mineral content. *Rock Mech. Rock Eng.* **2017**, *50*, 485–491. [CrossRef]
17. Ma, C.Q.; Li, H.Z.; Niu, Y. Experimental study on damage failure mechanical characteristics and crack evolution of water-bearing surrounding rock. *Environ. Earth Sci.* **2018**, *77*, 23. [CrossRef]
18. Liu, D.Q.; Wang, Z.; Zhang, X.Y.; Wang, Y.; Zhang, X.L.; Li, D. Experimental investigation on the mechanical and acoustic emission characteristics of shale softened by water absorption. *J. Nat. Gas Sci. Eng.* **2018**, *50*, 301–308. [CrossRef]
19. Liu, Y.L.; Wang, L.G.; Sun, X.K.; Wang, J. Experimental study of the influence of water and temperature on the mechanical behavior of mudstone and sandstone. *Bull. Eng. Geol. Environ.* **2017**, *76*, 645–660. [CrossRef]

20. Zhu, M.T.; Dai, Y.P.; Zhang, L.C.; Wang, C.L.; Liu, L. Geochronology and geochemistry of the Nanfen iron deposit in the Anshan-Benxi area, North China Craton: Implications for 2.55 Ga crustal growth and the genesis of high-grade iron ores. *Precambrian Res.* **2015**, *260*, 23–38. [CrossRef]
21. Zhu, C.; Tao, Z.G.; Yang, S.; Zhao, S. V shaped gully method for controlling rockfall on high-steep slopes in China. *Bull. Eng. Geol. Environ.* **2018**. [CrossRef]
22. Yang, X.J.; Hou, D.G.; Hao, Z.L.; Tao, Z.G.; Shi, H.Y.; Jin, K. Research on correlations between slope stability and rainfall of high steep slope on Nanfen open-pit iron ore. *Chin. J. Rock Mech. Eng.* **2016**, *35*, 3232–3240. [CrossRef]
23. Yang, X.J.; Hou, D.G.; Wang, J.M.; Wang, J.X. Study on the stability and remote real-time monitoring for high steep slope in Nanfen open pit iron mine. *J. Min. Saf. Eng.* **2017**, *34*, 1000–1007. [CrossRef]
24. Vinoth, S.; Kumar, L.A.; Kumar, E. Slope stability monitoring by quantification and behavior of microseismic events in an opencast coal mine. *J. Geol. Soc. India* **2015**, *85*, 450–456. [CrossRef]
25. Dai, Y.P.; Zhu, Y.D.; Zhang, L.C.; Zhu, M.T. Meso- and Neoarchean Banded Iron Formations and Genesis of High-Grade Magnetite Ores in the Anshan-Benxi Area, North China Craton. *Econ. Geol.* **2017**, *112*, 1629–1651. [CrossRef]
26. Chueasamat, A.; Hori, T.; Saito, H.; Sato, T.; Kohgo, Y. Experimental tests of slope failure due to rainfalls using 1g physical slope models. *Soils Found.* **2018**, *58*, 290–305. [CrossRef]
27. Li, Y.Y.; Zhang, S.C.; Zhang, X. Classification and fractal characteristics of coal rock fragments under uniaxial cyclic loading conditions. *Arab. J. Geosci.* **2018**, *11*, 201. [CrossRef]
28. Lee, J.S.; Yoon, H.K. Characterization of rock weathering using elastic waves: A Laboratory-scale experimental study. *J. Appl. Geophys.* **2017**, *140*, 24–33. [CrossRef]
29. Ding, P.B.; Di, B.R.; Wang, D.; Wei, J.X.; Zeng, L.B. P- and S-wave velocity and anisotropy in saturated rocks with aligned cracks. *Wave Motion* **2018**, *81*, 1–14. [CrossRef]
30. Amalokwu, K.; Best, A.I.; Sothcott, J.; Chapman, M.; Minshull, T.; Li, X.Y. Water saturation effects on elastic wave attenuation in porous rocks with aligned fractures. *Geophys. J. Int.* **2014**, *197*, 943–947. [CrossRef]
31. Wang, X.; Wen, Z.; Jiang, Y.; Huang, H. Experimental study on mechanical and acoustic emission characteristics of rock-like material under non-uniformly distributed loads. *Rock Mech. Rock Eng.* **2018**, *51*, 729–745. [CrossRef]
32. Lagoeiro, L.; Goncalves, C.C. SEM observation of grain boundary structures in quartz-iron oxide rocks deformed at intermediate metamorphic conditions. *Ann. Braz. Acad. Sci.* **2011**, *83*, 875–889. [CrossRef]
33. Berdnikov, N.V.; Konovalova, N.S.; Zazulina, V.Y. Investigation of precious metal inclusions in highly carbonaceous rocks by the SEM and X-Ray spectrum analysis methods. *Russ. J. Pac. Geol.* **2010**, *4*, 164–170. [CrossRef]
34. Xu, W.Y.; Zhang, Q.; Zhang, J.C.; Wang, R.B.; Wang, R.K. Deformation and control engineering related to huge landslide on left bank of Xiluodu reservoir, South-West China. *Eur. J. Environ. Civ. Eng.* **2013**, *17*, 249–268. [CrossRef]
35. Conte, E.; Troncone, A. A performance-based method for the design of drainage trenches used to stabilize slopes. *Eng. Geol.* **2018**, *239*, 158–166. [CrossRef]
36. Li, J.M.; Huang, Y.L.; Qiao, M.; Chen, Z.W.; Song, T.Q.; Kong, G.Q.; Gao, H.D.; Guo, L. Effects of water soaked height on the deformation and crushing characteristics of loose gangue backfill material in solid backfill coal mining. *Processes* **2018**, *6*, 64. [CrossRef]
37. Yang, X.J.; Hou, D.G.; Hao, Z.L.; Wang, E.Y. Fuzzy comprehensive caused by underground mining subsidence and its monitoring. *Int. J. Environ. Pollut.* **2016**, *59*, 284–301. [CrossRef]
38. Tao, Z.G.; Meng, X.Z.; Ma, C.R.; Zhu, C.; He, M.C.; Wang, C.J.; Zhang, H.J. Analysis of wedge-shaped landslide mechanism and sliding force monitoring warning in Nanfen open pit iron mine. *J. China Coal Soc.* **2017**, *42*, 3149–3158. [CrossRef]